International Journal of Engineering Research & Technology (IJERT)
ISSN: 2278-0181
Vol. 3 Issue 3, March - 2014

On Quasi-Newton Method Applied To 2D Wheel-Rail Contact Models

Crinela Pislaru, Arthur Anyakwo
University of Huddersfield, Institute of Railway Research
Huddersfield, United Kingdom

Abstract—**Reliable and proficient numerical methods are required to determine the contact points between wheel and rail. This paper presents the use of Quasi-Newton method for determining the solution of a reduced number of non-linear wheel-rail contact geometry equations that arise as a result of the interaction of wheel and rail on the track.**

A novel two dimensional (2D) wheel-rail contact model is developed by using the wheel-rail contact co-ordinates to calculate the wheel-rail normal contact forces without approximating the contact angle. The simulated results are stored in a lookup table and accessed during the simulation of the bogie dynamic behaviour thus reducing the computational time. The reduced number of non-linear wheel-rail contact geometry equations and employment of Quasi-Newton method enable the proposed 2D wheel-rail contact model to be used for fast and real time simulations of complex and non-linear wheel-rail contact mechanics.

Keywords—wheel-rail interface; lateral displacement; yaw angle; wheel-rail contact model; railway vehicle dynamics; normal forces

I. INTRODUCTION

Numerical iterative methods have been widely used for solving systems of multi-dimensional non-linear equations. Newton's methods [1] are widely used in most engineering problems (especially where accurate details of the system are known) due to the fast speed of convergence. However graphical methods should be employed to understand the system model and offer good guess for both single and multi-dimensional equation version. Newton-Raphson methods [1] exhibit a rather fast speed of quadratic convergence once the solution has been found. The major setbacks are the expensive computation of the Jacobian matrix for the solution of non-linear equations and the inability to make an initial guess.

Quasi-Newton methods [2] eliminate the need for the computation of the Jacobian at every time step. It is often preferable to store an approximation to the Jacobian rather than anapproximation to the inverse Jacobian for solving large systems of nonlinear equations. The updating procedure can be mademore efficient for the approximate Jacobian than for the approximate inverse Jacobianwhen the Jacobian issparse and the locations of the zeroes are known.This approximate Jacobian matrix is used to determine the solutions of the non-linear multidimensional equations which are so complex that their differentiation might not be practical. The computational time is reduced so it is possible to run the iteration in conjunction with other iterations and Quasi-Newton methods are used in the present paper to solve wheel-rail contact dynamics problems.

Wickens [3] solves the wheel-rail contact geometry equations using Newton Raphson's method. The wheel-rail contact co-ordinates are determined by taking into account the lateral displacement and the roll angle and then used for wheel-rail track simulations. But it is difficult to make an initial guess for solving the equations.Sugiyama and Suda [4] apply Newton Raphson's method to solve wheel-rail contact equations and determine the contact points by using the online contact search, offline contact search and hybrid contact search methods. They perform multibody railroad vehicle dynamics simulations using the elastic contact method and the hybrid method which combines the online and offline methods for the determination of the wheel-rail contact points. However experience of the actual wheel-rail contact geometry has to be used to choose the starting guess for the simulation process.

Anyakwo et al [5] develop a novel method for determining the contact positions of wheel-rail contact using the analytical non-iterative approach. The wheel and rail profiles are divided into various regions of contact and the equations relating the wheel movement and the rail are derived with the lateral displacement as input. Quasi-Newton's method is used to determine the wheel-rail contact geometry parameters which are saved in a look-up table. This technique does not require the contact position to be determined by adjusting the roll angle repeatedly until minimum difference between the wheel and the rail profile is achieved. The iterative approach is eliminated because the rolling radius difference change is negligible for very small changes in the lateral contact position. But the wheel and rail profile regions are switched repeatedly to determine the contact positions depending on the contact point regions thus making it very tedious to use especially for non-conical wheel profiles where the tread region is non-linear in shape. Also fourteen non-linear differential equations have to be solved synchronously which requires increased computational power.

Zheng and Wu [6] determine the solutions of the normal contact problem: normal contact forces, size, shape and orientation of the wheel-rail contact patch and normal pressure distribution along the contact patch area. Analytical techniques are used to determine the normal contact forces on the wheel tread region for the left and right wheel-rail contact assuming that for non-conformal contact condition exists and Hertz contact model is applied. This method is valid for the computation of the normal forces provided that the effect of the contact angles and the roll angles are small.

Iwnicki [7] presents an approximate analytical method for determining the wheel-rail contact normal forcesconsidering the effect of the contact angles: roll angle and yaw angle. The study shows that the computed normal contact forces at flange contact depend on friction coefficient, contact angle and yaw angle of the wheelset and the axle load. This method gives accurate predictions of the normal contact forces occurring at the flange contact region thus enabling yaw angle of the wheelset to be included in dynamic simulations.

This paper presents the use of Quasi-Newton method for determining the solution of a reduced number of non-linear differential equations of the wheel-rail contact geometry thus reducing the time required for dynamic simulations of the bogie on the railway track. Also this paper describes the development of a novel 2D wheel-rail contact model and the normal contact problem, tangential contact problem and wheel rail dynamic simulations are implemented to investigate the dynamic behaviour of a bogie on the track. Also the wheel-rail normal contact forces are calculated without approximating the contact angle.This non-iterative 2D wheel rail contact model is useful for studying wheelset derailment, prediction of wheel climb, wear predictions and lateral stability of the bogie on the track.

II. QUASI NEWTON METHOD

Computing the Jacobian matrix is very expensive especially if much of the work carried out is used in evaluating the function f. The Jacobian is therefore difficult to evaluate since it is computed using finite differences. Quasi Newton methods replace the true $f'(x_n)$ in the Newton Raphson equation in equation (1) by estimates which can be modelled from value function over the sequence of iterations.

In Quasi-Newton iteration method, the sequence of approximations is expressed by the equation similar to Newton Raphson method [2].

$$\{x_{n+1}\} = \{x_n\} - [J]^{-1}\{f\} \tag{1}$$

Where J is the jacobian matrix, f is the non-linear equation function and x_n is the variable.

The Quasi-Newton method can be expressed as:

$$x_{n+1} = x_n - \propto_n C_n f(x_n) \tag{2}$$

where $\propto_n$ is a complex number and matrix C_n represents the nth approximation of $J^{-1}(x^*)$. Introducing a metric into the residual space it yields:

$$\sigma_{n+1} = (f_{n+1}, f_{n+1}) = {f^T}_{n+1} N f_{n+1} \tag{3}$$

where ${f^T}_n$ is the transpose of f_n and the metric matrix N is the Hermitian which is independent of x and is positive or negative definite. The complex number, $\propto_n$ can be calculated to minimize the function σ_{n+1}. This leads to the non-linear equation of the form:

$$(f_{n+1},\ J_{n+1} C_n f(x_n)) = 0 \tag{4}$$

For the special case if G is a non-singular matrix, equation (4) is linear in $\propto_n$ and it gives:

$$\propto_n = \frac{-(G C_n f(x_n), f_n)}{(G C_n f(x_n), G C_n f(x_n))} \tag{5}$$

where C_n is equal to G^{-1} then equation (5) gives $\propto_n$ = 1 and we have the generic Newton's method. If we start with an initial estimate C_1we can write:

$$C_{n+1} = C_n + D_n \tag{6}$$

The matrix D_n can be determined and expressed as

$$D_n = \left[\frac{\beta_n {u_n}^T}{(u_n, \Delta f_n)} - \frac{C_n \Delta f_n {v_n}^T}{(v_n, \Delta f_n)}\right] N \tag{7}$$

The vectors u_n, and v_n are not yet determined. C_n can be expressed as follows because $i + 1 < n$:

$$C_n = C_{n+1} + \sum_{j=i+1}^{n-1} D_j \tag{8}$$

If the vectors u_n, and v_n are chosen such that they can be orthogonal to the subspace spanned by Δf_n $(i < n)$:

$$(u_n, \Delta f_n) = (u_n, \Delta f_n) = 0 \tag{9}$$

The convergence of the iteration expressed in equation (7), (8) and (9) can be used to solve a system of equations since the space of the residuals cannot exceed n because of the linearly independent vectors in the space. The matrix C_{n+1} can be structured assuming that Δf_n, $(i \le n)$. Thus since the vectors need to be orthogonal, a great deal of flexibility exists for different choices of u_n and v_n. One possible simplification of the quasi-Newton method is to express D_n as the follows:

$$D_n = (\beta_n - C_n \Delta f_n) \frac{{u_n}^T N}{(u_n, \Delta f_n)} \tag{10}$$

where $\beta_n = \propto_n C_n f(x_n)$

This value of the vectors u_n, and v_n can be used to obtain other quasi Newton methods for solving non-linear differential equations. For instance Powell algorithm [8] is one method that is used for calculating the unconstrained minimum (or maximum) of the quadratic function given by:

$$D_n = \frac{\beta_n {\beta_n}^T}{({\Delta f_n}^T \beta_n)} - \frac{C_n \Delta f_n \Delta f_n {u_n}^T C_n}{({\Delta f_n}^T, C_n \Delta f_n)} \tag{11}$$

Equation (11) defines the correction matrix proposed by Davidon-Fletcher-Powell [8]. This algorithm poses difficulties since problems occur in finding the constrained extremum. The modification suggested was found to be computationally unsatisfactory due to the round off errors obtained during the simulations. These errors are very large and thus lead to various problems. The most stable quasi Newton method that is stable to any system of equations that could be linear and nonlinear is the method proposed by Barnes presented by Rosen [18].Barnes algorithm defines D_n as follows:

$$D_n = (\beta_n - C_n \Delta f_n) \frac{z_n{}^T N C_n}{(z_n, C_n \Delta f_n)} \quad (12)$$

where z_n is obtained from β_n using Schmidt orthogonalization procedure presented in [18]. The first method assumes that z_n is equal to β_n. D_n is then expressed as follows:

$$D_n = (\beta_n - C_n \Delta f_n) \frac{\beta_n{}^T N C_n}{(\beta_n, C_n \Delta f_n)} \quad (13)$$

The disadvantage of using this algorithm is that it cannot be guaranteed that β_n will be orthogonal thus we can't be very sure of convergence. The second method proposed by Broyden [9] chooses $u_n = \Delta f_n$ to realize

$$D_n = (\beta_n - C_n \Delta f_n) \frac{\Delta f_n{}^T N}{(\Delta f_n, \Delta f_n)} \quad (14)$$

This suffers from problems that Δf_n will not be orthogonal is most cases. The problem can be solved if Δf_n does not lie near the solution [9].

III. WHEEL-RAIL CONTACT POINT DETERMINATION

Davidon-Fletcher-Powellderived above is used to solve the reduced set of non-linear differential wheel-rail contact equations in MATLAB. The wheel-rail contact geometry equations are derived from the wheel-rail contact geometry model that would be discussed shortly. The wheel-rail contact model used is the 2D wheel-rail contact model that considers the movement of the wheelset in two dimensions, the lateral displacement (u_y) and roll angle (ϕ) thus forming two degrees of freedom. The four wheel-rail contact co-ordinates of interest for each wheel-rail contact are the lateral wheel contact co-ordinate (Y_{wr}), lateral rail contact co-ordinate (Y_{rr}), vertical wheel contact co-ordinate $W(Y_{wr})$ and the vertical rail contact co-ordinate $R(Y_{rr})$ as shown in the figure below:

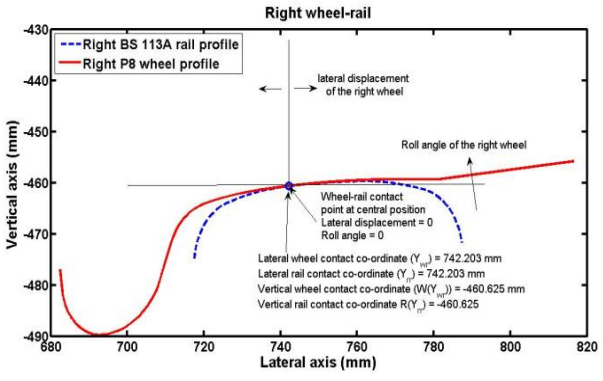

Figure 1. Right wheel-rail contact at central position

Similarly the contact positions at the left wheel-rail contact are the same but the lateral co-ordinates are negative since it is on the negative axis of the wheel-rail contact.

The inputs for the proposed 2D wheel-rail contact geometry are the lateral displacement (u_y), the roll angle (ϕ) and the piecewise cubic interpolation of the wheel and the rail profiles. The standard new P8 wheel profile [13] and BS 113A rail profile [14] are used to develop the wheel-rail contact model.

The fixed frame of reference shown in Figure 2 defines the contact point location with respect to the wheelset frame centre of mass. This means that the co-ordinates at the wheelset centre is $A_fO_fB_f$ (0,0). The co-ordinate at the right wheel contact with respect to the fixed reference frame is (Y_{wr}, $-W(Y_{wr})$) while the co-ordinates at the left wheel contact is (Y_{wl}, $-W(Y_{rl})$).

Table 1.1 shows the co-ordinates of the right/left wheel-rail profiles at central position

Table 1.1. Wheel-rail contact co-ordinates at central position

Right wheel-rail profile		Left wheel-rail profile	
Ywr = Yrr	**W(Ywr) = R(Yrr)**	**Ywl = Yrl**	**W(Ywl) = R(Yrl)**
742.203 mm	-460.625 mm	-742.203 mm	-460.625 mm

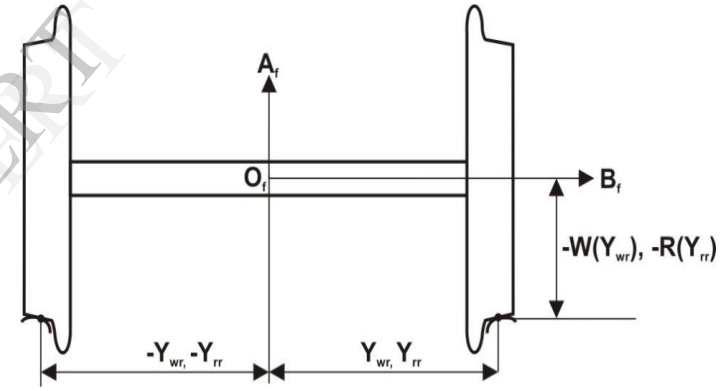

Figure 2. Fixed frame of reference $A_fO_fB_f$

The kinematic equation describing the contact point location on the wheel and rail interface is:

$$P^{railj} = U^{rail}_{wheel} + A(\phi) P^{wheelj} \quad (15)$$

where P^{railj} is a generic point on the rail profile, U^{rail}_{wheel} defines the movement of the wheelset in the vertical and lateral direction, $A(\phi)$ is the rotation matrix, and P^{wheelj} is a generic point on the wheelset with respect to the Fixed reference frame and j represents the left (l) or right (r). The rotation matrix is a function of the roll angle and is defined as the rotation of the wheelset about the longitudinal direction of motion. It can be expressed as follows:

$$A(\phi) = \begin{bmatrix} cos\phi & -sin\phi \\ sin\phi & cos\phi \end{bmatrix} \quad (16)$$

While co-ordinates of the wheelset centre of mass is:

$$U_{wheel}^{rail} = \begin{bmatrix} u_y \\ u_z \end{bmatrix} \quad (17)$$

The position of a point on the right rail profile is:

$$P^{railr} = \begin{bmatrix} Y_{rr} \\ R(Y_{rr}) \end{bmatrix} \quad (18)$$

While the position of a point on the right wheel profile is:

$$P^{wheelr} = \begin{bmatrix} Y_{wr} \\ W(Y_{wr}) \end{bmatrix} \quad (19)$$

Substituting Equation (16) to (19) into Equation (15) and

$$Y_{rr} = u_y + Y_{wr}\cos\phi - W(Y_{wr})\sin\phi \quad (20)$$

$$R(Y_{rr}) = u_{zr} + Y_{wr}\sin\phi + W(Y_{wr})\cos\phi \quad (21)$$

expanding the expression we have:

Similarly, the equations for the left wheel-rail contact geometry can be represented as thus; the position of a point on the left rail profile is defined as:

$$P^{raill} = \begin{bmatrix} Y_{rl} \\ R(Y_{rl}) \end{bmatrix} \quad (22)$$

While the position of a point on the left wheel profile is:

$$P^{wheell} = \begin{bmatrix} Y_{wl} \\ R(Y_{wl}) \end{bmatrix} \quad (23)$$

Substituting Equation (22) to (23) into Equation (15) and

$$Y_{rl} = u_y + Y_{wl}\cos\phi - W(Y_{wl})\sin\phi \quad (24)$$

$$R(Y_{rl}) = u_{zl} + Y_{wl}\sin\phi + W(Y_{wl})\cos\phi \quad (25)$$

expanding the expression we have:

Equations (20) and (21) contain three unknown variables,Y_{rr}(lateral contact point on the right rail profile),Y_{wr}(Lateral contact position of the right wheel profile) and u_{zr} (vertical displacement at the right wheel) while equations (24) and (25) containY_{rl} (lateral contact point on the left rail profile), Y_{wl} (lateral contact point on the right wheel profile) and u_{zl} (vertical displacement at the right wheel). $W(Y_{wl})$ is the left wheel rolling radius while $W(Y_{wr})$ is the right wheel rolling radius, u_y is the rolling radius and ϕ is the roll angle of the wheelset.

The three unknown variables included in the equations for the right and left wheel can be reduced to two unknown variables by substituting Equation (20) into Equation (21) and Equation (24) into Equation (25) as follows:

$$R\left(u_y + Y_{wr}\cos\phi - W(Y_{wr})\sin\phi\right) = u_{zr} + Y_{wr}\sin\phi + W(Y_{wr})\cos\phi \quad (26)$$

$$R\left(u_y + Y_{wl}\cos\phi - W(Y_{wl})\sin\phi\right) = u_{zl} + Y_{wl}\sin\phi + W(Y_{wl})\cos\phi \quad (27)$$

The wheel and rail profileshave to touch each other only in one contact point location thus fulfilling the non-conformal condition with no interpenetration[1]. For this to be satisfied the tangents to the wheel and rail profile planes must be determined by differentiating Equation (26) with respect toY_{wr} and Equation (27) with respect to Y_{wl}. This yields:

$$R'\left(u_y + Y_{wr}\cos\phi - W(Y_{wr})\sin\phi\right)\left(\cos\phi - W'(Y_{wr})\right) - \sin\phi + W'(Y_{wr})\cos\phi = 0 \quad (28)$$

Similarly for the left wheel-rail contact the tangent to the wheel and rail profile plane can be found by differentiating Equation (27):

$$R'\left(u_y + Y_{wl}\cos\phi - W(Y_{wl})\sin\phi\right)\left(\cos\phi - W'(Y_{wl})\right) - \sin\phi + W'(Y_{wl})\cos\phi = 0 \quad (29)$$

Equation (26) to (29) can then be solved using Quasi Newton's to determine the four unknownsY_{wr} ,u_{zr} , Y_{wl}, u_{zl} for given inputs u_y andϕ. The error difference between the vertical displacements of the right and left wheel must be less than 1x10^{-6}mm to ensure that u_{zr} is approximately equal to u_{zl}.

Figure 3 contains the block diagram showing the steps of the novel algorithm proposed to solve the wheel-rail contact geometry equations (26 – 29).

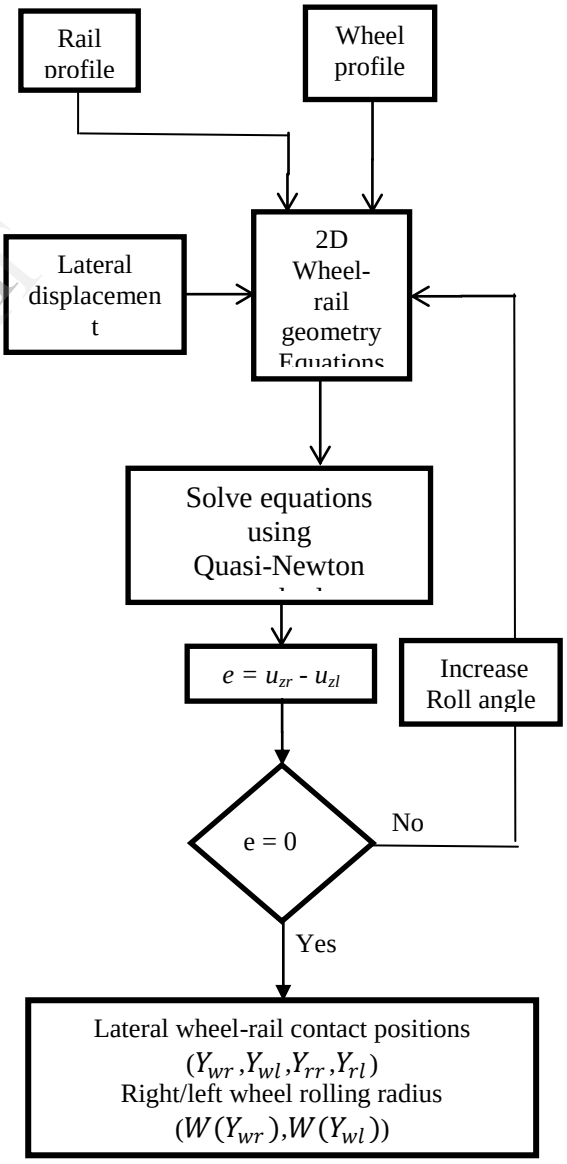

Figure 3. Block diagram algorithm for the wheel-rail contact geometry

The outputs of the block diagram which include the lateral wheel-rail contact positions, right/left wheel rolling radius and the wheel-rail contact angle are used in wheel-rail contact model to investigate the dynamic behaviour of the bogie on the railway track. The contact point locations on BS 113A and P8 wheel profiles are determined using the block diagram and can be shown in Figure 4and Figure 5 below;

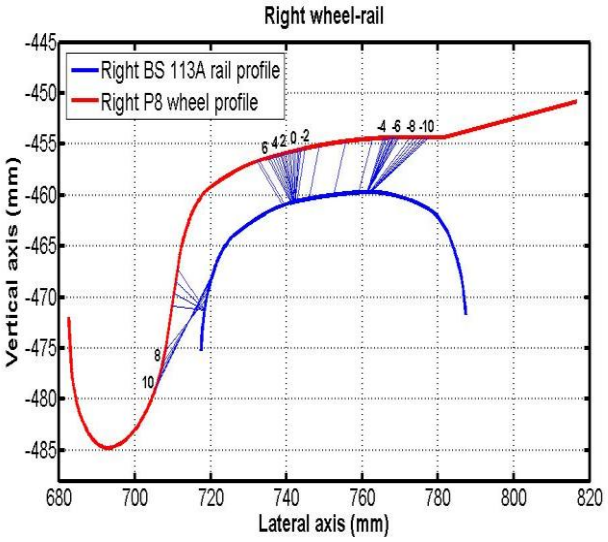

Figure 4. Right wheel-rail contact positions (Positive/Negative lateral displacement)

Figure 4 shows that a significant jump is noticed from 6 mm to 8 mm because the right wheel has reached the flange region. Also for negative lateral displacement, the contact jump is observed from 2 mm to 4 mm due to the rail and wheel-geometry and the rail cant angle.

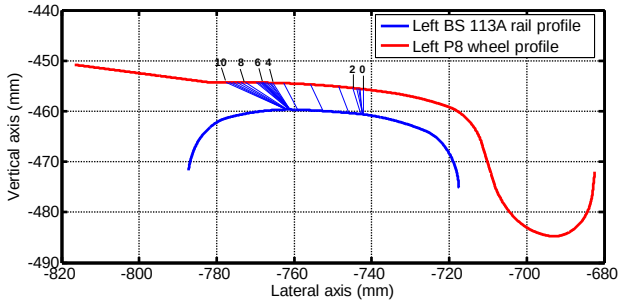

Figure 5. Left wheel-rail contact positions (Positive/Negative lateral displacement)

It can be observed from Figure 4 that there are significant contact point jump from 2 mm to 4 mm due to the wheel profile design and the rail geometry.

3.1. Wheel-rail contact geometry results

Figure 5 shows the results obtained for the right and left wheel-rail contact positions

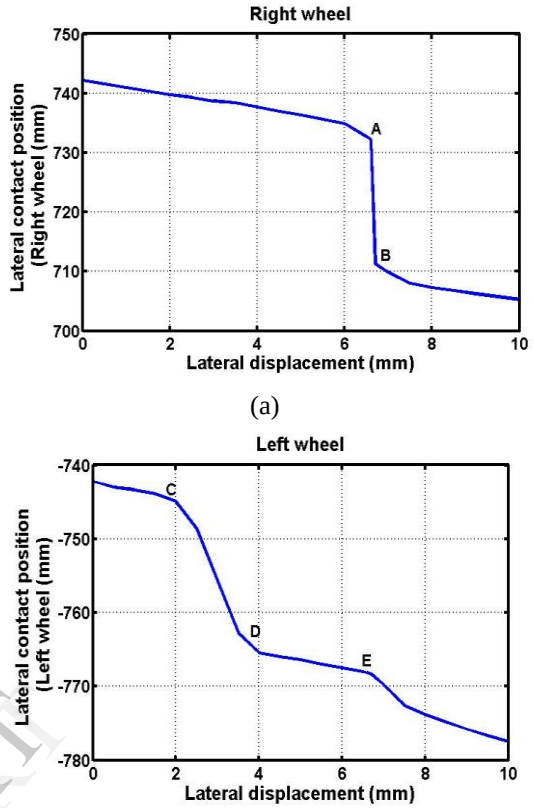

Figure 6: Right (a) and Left (b) lateral wheel contact positions

There is a contact point jump in the right wheel lateral contact position between points A and B because the right wheel has reached the wheel flange region. For the left wheel, two contact jumps are observed in the lateral left wheel contact position from C to D and from D to E. This is as a result of the cant angle of the rail profile and the geometry of the wheel profile at those regions.

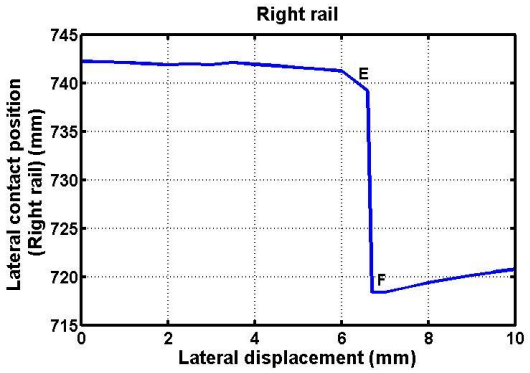

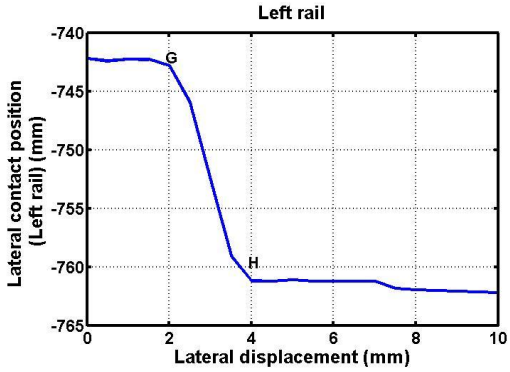

(b)

Figure 7. Right (a) and Left (b) lateral rail contact positions

Figure 7 shows the contact point location of the right and left rail contact position as a function of the lateral displacement. Results show that for lateral displacement range of 6.5 mm to about 6.8 mm the contact point position jumps from E to F. This indicates that the wheelset has reached the rail gauge region of the right rail as a result of flange contact. Similarly the rail contact point location jumped from G to H for 2 mm to 4 mm range as a result of the cant angle of the rail profile at that region.

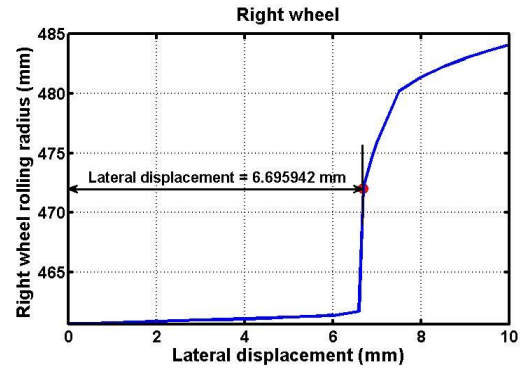

(a)

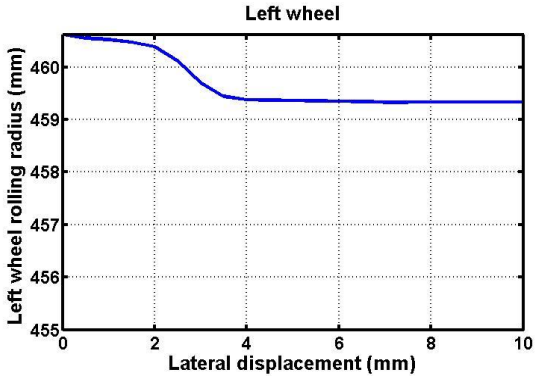

(b)

Figure 8. Right (a) and left (b) wheel rolling radius

Figure 8 shows the rolling radius of the left right and left wheel. The rolling radius of the right wheel increase slowly with increasing lateral displacement in the wheel tread region and then increases sharply after 6.5 mm until it gets to flange contact at 6.695942 mm. Also the left wheel rolling radius also shows significant decrease in the rolling radius for lateral displacement range 2 mm to 4 mm as a result of the rail profile geometry.

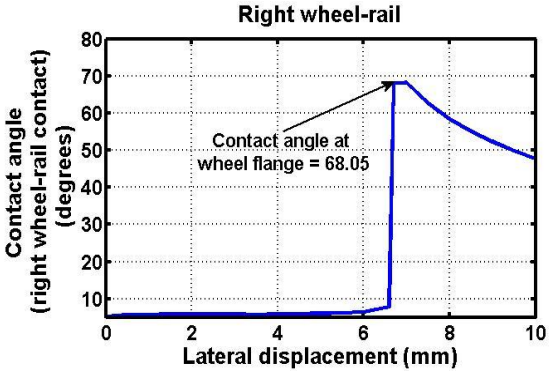

(a)

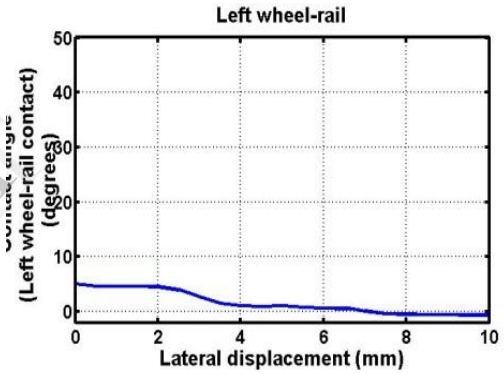

(b)

Figure 9. Right (a) and left (b) wheel contact angle

Figure 9 represents the right wheel and left wheel contact angle for lateral displacement range of 0 mm to 10 mm. A sharp increase in right contact angle occurs at lateral displacement near the flange region as a result of right flange/rail gauge contact. The maximum contact angle at flange contact is 68.05 degrees. The contact angle can be mathematicallyexpressed as by the following expression:

$$\delta_{rR} = arctan\left(\frac{dR(Y_{rR})}{dY_{rR}}\right), \qquad \delta_{rL} = arctan\left(\frac{dR(Y_{rL})}{dY_{rL}}\right) \tag{30}$$

Figure 9 displays the rolling radius difference function obtained by subtracting the rolling radius of the left wheel from the right wheel.

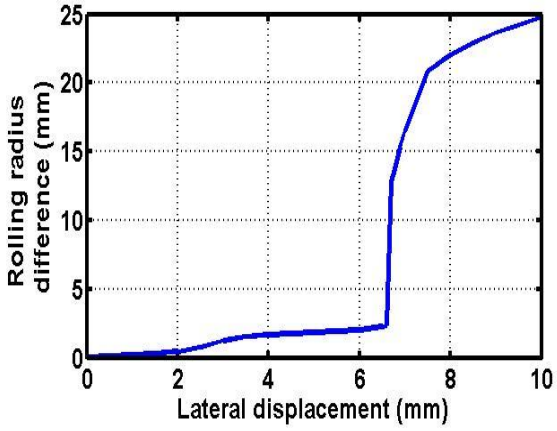

Figure10. Rolling radius difference function

The rolling radius difference in Figure 10 was obtained by finding the difference between the right wheel and the left wheel rail contact. The Rolling Radius Difference (RRD) is expressed as follows

$$RRD(y) = W(Y_{WR}) - W(Y_{WL}) \tag{31}$$

The wheel-rail contact co-ordinates Y_{wr}, Y_{rr},$W(Y_{wr})$, $R(Y_{rr})$ have been determined using Quasi-newton method. The are saved in a look-up table and used for dynamic simulations. This offers advantages over the iterative methods whereby the wheel-rail contact points are determined for each lateral displacement and used for dynamic simulations.

IV. NORMAL CONTACT PROBLEM

The normal contact problem resolves the vertical and normal contact forces acting on the wheel-rail contact. The wheel-rail contact forces are derived by analyzed the creep forces developed on the wheel-rail contact. Figure 11 shows the wheel-rail contact forces acting on the wheelset.

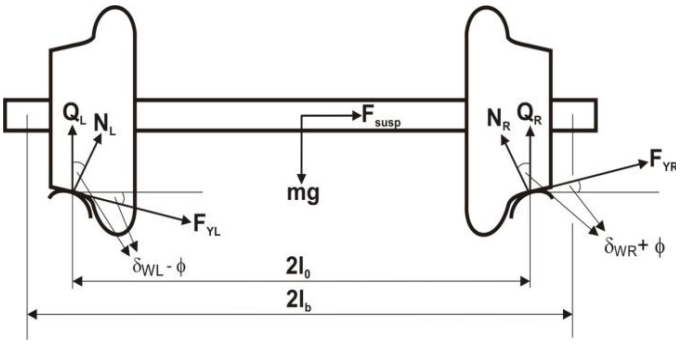

Figure 11. Wheel-rail interaction forces on the wheelset

The equation of motion of the wheelset in the lateral direction is expressed as follows:

$$F_{YR}\cos(\delta_{rR}) + F_{YL}\cos(\delta_{rl}) - N_R\sin(\delta_{rR}) + N_L\sin(\delta_{rl}) + F_{SUSP} = 0 \tag{32}$$

where

$$\delta_{rR} = \delta_{wR} + \phi, \quad \delta_{rl} = \delta_{wl} - \phi, \tag{33}$$

where F_{YR} is the lateral creep force developed at the right wheel-rail, F_{YL} is the lateral creep force developed at the left wheel wheel-rail contact, *Fsusp* is the lateral suspension force.

In the vertical direction for the right wheel-rail contact vertical forces can be expressed as follows;

$$\left(F_{YR}\sin(\delta_{rr}) + N_R\cos(\delta_{rr})\right) - Q_R = 0 \tag{34}$$

Similarly, for the left wheel-rail contact the vertical forces can be resolved as follows;

$$\left(-F_{YL}\sin(\delta_{rl}) + N_L\cos(\delta_{rl})\right) - Q_L = 0 \tag{35}$$

Where Q_R and Q_L are the right and left vertical forces applied on the wheel-rail contact respectively. The can be expressed as follows [6]:

$$Q_R = \frac{W}{2} + \frac{F_{SUSP}W(Y_{WL})}{(2l_b - \Delta_R + \Delta_L)} + \frac{mg(l_b + \Delta_L)}{(2l_b - \Delta_R + \Delta_L)} \tag{36}$$

$$Q_L = \frac{W}{2} - \frac{F_{SUSP}W(Y_{WR})}{(2l_b - \Delta_R + \Delta_L)} + \frac{mg(l_b - \Delta_R)}{(2l_b - \Delta_R + \Delta_L)} \tag{37}$$

Where W is the wheelset axle weight, l_b is the half length of the longitudinal spring, Δ_R and Δ_L are the distances from the right and left nominal contact positions, m is the mass of the wheelset, and g is the acceleration due to gravity.

Let i = L, R, then applying Kalker's linear theory, the longitudinal (F_{Xi}), lateral (F_{Yi})and spin moment (M_{Zi}) creep forces developed at the wheel-rail contact can be expressed as follows:

$$F_{Xi} = -f_{11}v_{Xi}, \quad F_{Yi} = -f_{22}v_{Yi} - f_{23}v_{SPINi}, \quad M_{Zi} = -f_{23}v_{Yi} - f_{33}v_{SPINi} \tag{38}$$

The longitudinal (v_{Xi}), lateral (v_{yi}) and spin (v_{SPINi}) creepages developed in the contact patch as a result of traction and braking can be defined as follows:

$$v_{Xi} = \left(1 - \frac{W(Y_{Wi})}{R_0}\right) \pm \frac{l_0}{v}\frac{d\psi}{dt}, \quad v_{yYi} = \frac{dy}{vdt} - \psi\cos(\delta_{ri}), \quad v_{SPINi} = \frac{d\psi}{vdt} \pm \frac{\sin(\delta_{ri})}{R_i} \tag{39}$$

where ψ is the yaw angle, and ± indicates the signs for the calculating the creepages. A positive signifies calculation of creepages for the left wheel-rail contact while the negative sign indicates calculation of creepages for the right wheel-rail contact. The longitudinal (f_{11i}), lateral (f_{22i}), lateral/spin (f_{23i}) and spin (f_{33i}) linear creep coefficients as proposed by Kalker by be defined as:

$$f_{11i} = Ga_ib_iC_{11i}, f_{22i} = Ga_ib_iC_{22i}, \quad f_{23i} = G(a_ib_i)^{1.5}C_{23i}, \quad f_{33i} = G(a_ib_i)^2C_{33i} \tag{40}$$

where G is the modulus of rigidity of the wheel and rail materials given as:

$$G = \frac{E}{2(1+a)} \tag{41}$$

E is the Young modulus of steel equal (207GPa) and a is Poisson's ratio equal to 0.33 [12], [13]. C_{11i},C_{22i},$C_{23i}$and C_{33i} are the longitudinal, lateral, lateral/spin creep and spin coefficients respectively. They depend on the Poisson's ratio, a and the ratio of the semi-axes of the contact patch a_i, b_i which represent the longitudinal and lateral semi-axes of the contact patch ellipse. They can be expressed as follows:

$$a_i = m_i \left[\frac{3(1-a^2)}{2E(A_i+B_i)} N_i\right]^{1/3},$$

$$b_i = n_i \left[\frac{3(1-a^2)}{2E(A_i+B_i)} N_i\right]^{1/3},\ A_i + B_i = 0.5\left(\frac{1}{R_{Ri}} + \frac{1}{W(Y_{Wi})}\right) \quad (42)$$

$R_{Ri}$is the principal transverse radii of curvature for the rail profile while $R_i$is the principal radi of curvature for the wheel profile.

Substituting a_i and $b_i$from equation (42) into equation (40), equation (40) into equation (38) and equation (38) into the equation (34) whereby i = L or R yields:

$$F_{Yi} = D_{22i} N_i^{2/3} + D_{23i} N_i \quad (43)$$

where

$$D_{22i} = -G m_i n_i \left[\frac{3(1-v^2)}{2E(A_i+B_i)}\right]^{2/3} C_{22i} v_{Yi} \quad (44)$$

$$D_{23i} = -G(m_i n_i)^{3/2} \left[\frac{3(1-v^2)}{2E(A_i+B_i)}\right] C_{23i} v_{SPINi} \quad (45)$$

The normal contact forcesdeveloped on the right and left wheel can be solved using Quasi Newton method by substituting Equation (43) into Equation (34) or (35) to obtain the expression:

$$(D_{22i} N_i^{2/3} + D_{23i} N_i)\sin(\delta_{ri}) + N_i \cos(\delta_{ri}) - Q_i = 0 \quad (46)$$

It is important to note that an initial guess is required for the normal contact forces of the right and left wheel rail contact for a feasible solution to be found. The starting guess is usually at the initial normal load of the wheel at central position. The simulation time required for computing the normal force is reduced since the wheel-rail contact co-ordinates have already been saved in a look-up table and hence are easily accessible for the calculation of the normal force and hence for dynamic simulations of the bogie on the track.

The wheel-rail contact problem is non-linear hence using a linear theory to relate the creep force-creepage leads to errors due to the non-linear geometric functions and the adhesion limits. The heuristic non-linear model computes the creep forces at the linear and non-linear region of the creep force creepage curve. It includes the effect of spin creepage of which is neglected in Johnson and Vermeulen. The theory of heuristic non-linear creep force model is discussed in [14], [15] and is used to calculated the tangential creep forces developed at the wheel-rail contact.

The equations of motion describing the movement of the bogie on the track can be implement by summing all the lateral forces and spin creep moment forces. Newton's law is then applied to solve all the equations acting on the vehicle. Details of the equations of motion of the bogie on the railway track can be found in [16]. Details of the calculations of the primary suspensions of wheelset 1 (F_{susp1}) and wheelset 2 (F_{susp2}) and the suspension moments of wheelset 1(M_{susp1}) and wheelset 2 (M_{susp2}) can be found in [16].

V. NUMERICAL SIMULATION RESULTS

For application purposes the saved wheel-rail contact geometry co-ordinates; the rolling radius, contact angle, roll angle and lateral wheel-rail co-ordinates was used to perform dynamic simulations of a single bogie running on a straight track. The bogie and the wheelset considered here are from the Manchester benchmark bogie used in British Rail Mark IV trains in the U.K. The parameters used for the simulation of the bogie model can be found in [16]. Figure 12 below shows the lateral behaviour of the front wheelset for forward speeds 10, 30, and 50 m/s using Heuristic non-linear method.

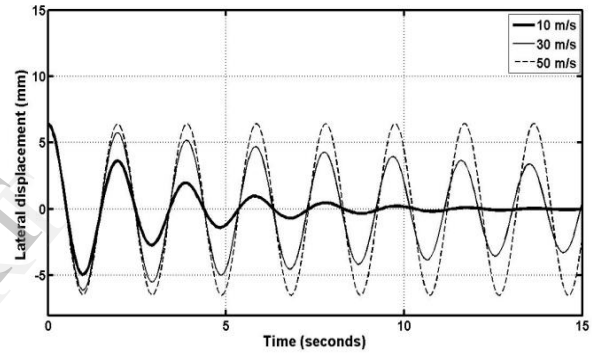

Figure 12. Lateral displacement of the front wheelset of the bogie for forward speeds 10m/s, 30 m/s and 50 m/s.

For forward speeds of 10 m/s and 30 m/s it can be observed that for the initial lateral misalignment of the front wheelset at 0.005 m decays and then returns to its central position on the track at nearly zero lateral displacement. As the velocity of the wheelset is increased from 10 m/s to 30 m/s and then 50 m/s the lateral oscillations increases and finally saturates at 50 m/s leading to hunting. For a velocity of 50 m/s the hunting motion has a null decaying rate hence the lateral behaviour of the wheelset shows harmonic oscillation. Hence the critical speed of the bogie model is 50 m/s or 180 km/hr.

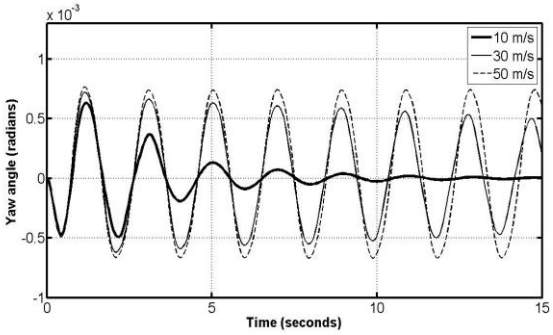

Figure 13. Yaw angle of the front wheelset of the bogie for forward speeds 10m/s, 30 m/s and 50 m/s.

Figure 13 shows the yaw angle of the front wheelset of the bogie for speeds, 10 m/s, 30 m/s and 50 m/s. For low forward speed 10 m/s the yaw angle response decays with time and settles to about zero radians, thus indicating that the front wheelset has returned to its central position. As the speed increases the yaw angle amplitude oscillations increase significantly. At 50 m/s hunting is observed which is similar to the lateral displacement of the wheelset.

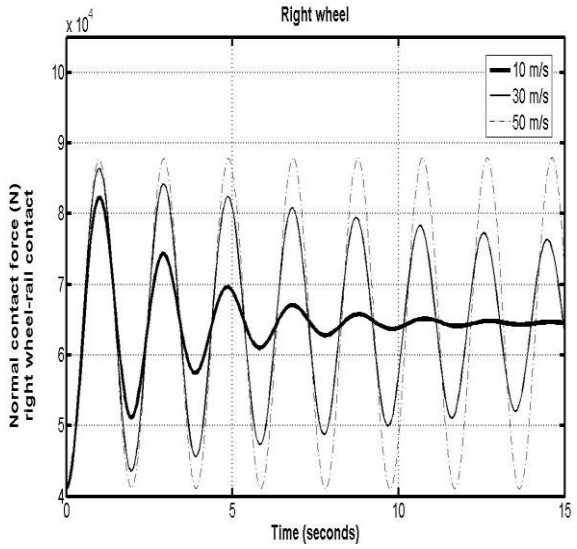

Figure 14. Normal contact force developed on the front wheelset for a forward speed of 10 m/s, 30 m/s and 50 m/s**.**

Figure 14 shows the normal contact force response of the front wheelset at forward speeds 10 m/s, 30 m/s and 50 m/s. The normal contact force decays at low speed with respect to time and settles at the central position at about 64 kN. For high forward speeds hunting occurs which show sustained oscillations of the normal forces. This indicates that critical speed of the bogie has been reached. The simulation time is reduced since the since the saved wheel-rail contact co-ordinates are stored offline and used to the simulation of dynamic movement of the wheel-rail contact in the system. In most iterative procedures for determining the wheel-rail contact, the wheel-rail contact points are determined online and used for dynamic simulations of the bogie on the track. This slows down the computation time since at every time step the wheel-rail contact point must be determined.

VI. CONCLUSIONS

This paper presents the use of Quasi-Newton method for determining the solution of a reduced number of non-linear wheel-rail contact geometry equations that arise as a result of the interaction of wheel and rail on the track. The simulation time is reduced since the since the saved wheel-rail contact co-ordinates are stored offline and used to the simulation of dynamic movement of the wheel-rail contact in the system. In most iterative procedures for determining the wheel-rail contact, the wheel-rail contact points are determined online and used for dynamic simulations of the bogie on the track. This slows down the computation time since at every time step the wheel-rail contact point must be determined. A novel two dimensional (2D) wheel-rail contact model is developed by using the wheel-rail contact co-ordinates to calculate the wheel-rail normal contact forces without approximating the contact angle. The simulated results have been stored in a lookup table and accessed during the simulation of the bogie dynamic behaviour thus reducing the computational time. The reduced number of non-linear wheel-rail contact geometry equations and employment of Quasi-Newton method enable the proposed 2D wheel-rail contact model to be used for fast and real time simulations of complex and non-linear wheel-rail contact mechanics and advanced condition monitoring systems for railway vehicles.

The wheel-rail contact co-ordinates geometry determined using a reduced number of non-linear wheel-rail geometry equations have been investigated using Quasi-Newton's method. The usage of Quasi-Newton method is investigated for the solution of the non-linear wheel-rail contact geometry equations that arise as a result of the interaction of the wheel and the rail on the track. The results indicate that the Quasi-Newton method provides an efficient solution strategy for the determination of the wheel-rail contact co-ordinates. The wheel-rail normal contact forces are then calculated without approximating the contact angle. The results of the simulations in are stored in a lookup table and accessed during the dynamic analysis of bogies thus reducing the computational time. The process of solving the ordinary differential equations representing the bogie dynamic behaviour becomes faster by using the lookup table. The simulation time is reduced since the since the saved wheel-rail contact co-ordinates are stored offline and used to the simulation of dynamic movement of the wheel-rail contact in the system. In most iterative procedures for determining the wheel-rail contact, the wheel-rail contact points are determined online and used for dynamic simulations of the bogie on the track. This slows down the computation time since at every time step the wheel-rail contact point must be determined.

The developed novel 2D wheel rail contact model is useful for studying wheelset derailment, prediction of wheel climb, wear predictions and lateral stability of the bogie on the track. The critical velocity of the bogie model using Heuristic non-linear model is 50 m/s. The proposed 2D wheel-rail contact model could be used for fast and real-time simulations of complex and nonlinear wheel-rail contact mechanics.

REFERENCES

[1] P. Kornerup and J.-M. Muller, "Choosing starting values for certain Newton–Raphson iterations," *Theoretical Computer Science*, vol. 351, no. 1, pp. 101–110, Feb. 2006.

[2] F. J., Zeleznik, "Quasi-Newton Methods for Nonlinear Equations", Journal of the association for Computing Machinery, Vol. 15, No. 2, pp. 265-271, 1968.

[3] A.H. Wickens, *Fundamentals of Rail Vehicle Dynamics*, 1st ed. Taylor & Francis, 2007.

[4] H. Sugiyama and Y. Suda, 'On the Contact Search Algorithms for Wheel/Rail Contact Problems', *Journal of Computational and Nonlinear Dynamics*, vol. 4, no. 4, p. 041001, 2009.

[5] A. Anyakwo, C. Pislaru, and A. Ball, 'A new method for modelling and simulation of the dynamic behaviour of the wheel-rail contact', *International Journal of Automation and Computing*, vol. 9, no. 3, pp. 237–247, Jul. 2012.

[6] J. Zeng and P. Wu, 'Study on the wheel/rail interaction and derailment safety', *Wear*, vol. 265, no. 9–10, pp. 1452–1459, Oct. 2008.

[7] S. Iwnicki, 'Simulation of wheel–rail contact forces', *Fatigue & Fracture of Engineering Materials & Structures*, vol. 26, no. 10, pp. 887–900, 2003.

[8] Powell, M. J. D., "A Fortran Subroutine for Solving Systems of Nonlinear Algebraic Equations," Numerical Methods for Nonlinear Algebraic Equations, Ch.7, 1970.

[9] Broyden, C. G., "A Class of Methods for Solving Nonlinear Simultaneous Equations". *Mathematics of Computation* (American Mathematical Society) 19 (92): 577–593, 1965.

[10] J. Sinclair, 'Feasibility of reducing the number of standard wheel profile designs', Railway Safety & Standard Boards, ITLR/T11299/001, Aug. 2002.

[11] BS1, 'British Standard Specification for Railways', BS 11:1985, Jul. 2004.

[12] J. Bhaskar, K. L. Johnson, and J. Woodhouse, 'Wheel-rail dynamics with closely conformal contact Part 2: Forced response, results and conclusions', *Proceedings of the Institution of Mechanical Engineers, Part F: Journal of Rail and Rapid Transit*, vol. 211, no. 1, pp. 27–40, Jan. 1997.

[13] Y. Gharaibeh, C. Ennaceur, P. Mudge, and W. Balachandran, 'Modelling guided waves in complex structures - Part 1: Rail', presented at the Non-Destructive Testing (NDT) conference, 2009, Blackpool, UK,, Blackpool, UK,.

[14] A. A. Shabana, K. E. Zaazaa, and H. Sugiyama, *Railroad Vehicle Dynamics: A Computational Approach*. Taylor & Francis, 2007.

[15] S.-Y. Lee and Y.-C. Cheng, 'A New Dynamic Model of High-Speed Railway Vehicle Moving on Curved Tracks', *Journal of Vibration and Acoustics*, vol. 130, no. 1, p. 011009, 2008.

[16] A. Anyakwo, C. Pislaru, A. Ball, and F. Gu, 'Modelling and simulation of dynamic wheel-rail interaction using a roller rig', *Journal of Physics: Conference Series*, vol. 364, p. 012060, May 2012.

[17] M. S. Engelman, G. Strang and K.-J. Bathe, "The application of quasi Newton methods in fluid mechanics, International Journal for Numerical Methods in Engineering Volume 17, Issue 5, May 1981, Pages: 707–718.

[18] Rosen, E. M., A review of quasi-Newton methods in nonlinear equation solving and unconstrained optimization. Proc, 21st Nat. Conference of the ACM. Thompson Book Co., Washington, D. C. 1966, pp. 37-41.